

## Discharge studies with a high efficiency XeCl-excimer laser

M. Trentelman, G.B. Ekelmans, F.A. van Goor and W.J. Witteman

University of Twente, Department of Applied Physics  
P.O. Box 217, 7500 AE Enschede, The Netherlands

### ABSTRACT

Results on a high efficiency excimer laser operating according to the prepulse-mainpulse technique<sup>1)</sup> are reported. The laser volume of about 90 cm<sup>3</sup> is X-ray preionized. The mainpulse obtained from a PFN is switched onto the discharge by means of a racetrack saturable inductor (magnetic switching)<sup>2),3),4)</sup> connected to the laser head with low inductance. Laser output energy has been measured as a function of gas mixture and delay between X-ray and prepulse.

### 1. INTRODUCTION

For scaling up of gas discharge excimer lasers to higher powers and higher repetition rates it is necessary to obtain a good understanding of the high pressure gas discharge laser at single shot operation. In order to do careful measurements to investigate the influence of different parameters, a highly reproducible discharge circuit is needed. In our case we used the prepulse-mainpulse excitation scheme with thyratrons as the active switches and a magnetic switch as a fast transfer switch for the mainpulse. In this way jitter could be reduced to less than 10 ns.

### 2. EXPERIMENTAL SETUP

The laser used in the experiments is shown in cross section in fig. 1. The laser-chamber is a stainless steel vessel suited for pressures up to 15 bar. A 60 cm long high-voltage electrode of Ni coated aluminium is mounted above a ground electrode made of a perforated stainless steel plate. The gap between the electrodes is 1.5 cm. The discharge volume of about 90 cm<sup>3</sup> is preionized by a cold-cathode X-ray source. The cathode (made of carbon felt) is separated 2 cm from a Ta-foil anode operating in the transmission mode. The Ta-foil is mounted on an aluminium plate which separates the high-pressure laser-chamber from the evacuated X-ray source. The e-beam diode is connected to the secondary of a pulse-transformer (7x). The primary circuit consist of a capacitor which is discharged by a EEV CX1154 thyatron through the primary winding of the pulse transformer. In this way a voltage pulse with a peak of about -100 kV and FWHM of 300 ns was delivered to the cathode. The electrical circuit connected to the high-voltage electrode is also shown in fig. 1 and in more detail in fig. 2.

Peaking capacitors amounting to a total capacitance of 6.4 nF are situated directly above the laserhead. A low impedance PFN is separated from the peaking capacitors by a race-track of CMD 5005 ferrite bricks. This race-track serves as a magnetic switch and switches the total discharge energy with a very fast risetime. In order to achieve fast switching the hysteresis loop of the race-track material should be almost rectangular with  $\Delta B$  as large as possible. Furthermore the total inductance between the PFN and the laserhead should be minimal when the race-track is saturated.

### 3. PRINCIPLE OF OPERATION

Typical waveforms for the prepulse-mainpulse excitation scheme are shown in fig. 3. The PFN is pulse-charged to  $V_m$  in about 6  $\mu$ sec from a storage capacitor  $C_s$ .  $C_s$  is discharged by a EEV

CX1159 thyratron through a 1:1 transformer (necessary for reversal of polarity). During the charging of the PFN the race-track is pulse reset to obtain a full flux swing. Just before the PFN is fully charged the prepulse is switched. The prepulse circuit is a classical C-L-C inversion circuit which charges the peaking capacitors (in a few tens of a nanosecond) to  $-V_p$ .

At this time the magnetic switch saturates and the voltage across  $C_p$  rapidly increases from  $-V_p$  to  $(2V_m + V_p)$  initiating a rapid avalanche breakdown of the laser gas, which is preionized by the X-ray source triggered just before the prepulse. The voltage across  $C_p$  will never reach  $2V_m + V_p$  because the impedance has dropped sufficiently for current flow through the laser to start and the voltage will drop to the steady state value  $V_{ss}$ .

For high efficiency operation  $V_m = 2V_{ss}$ ;  $V_p \sim 2V_{ss}$ . In this case the electrical efficiency for energy transfer from the PFN into the discharge is maximum.

#### 4. RESULTS

Fig. 4 shows the dependence of the efficiency of the laser on the partial pressure of HCl for two different partial pressures of Xenon. The buffer-gas is 4 bar of Neon. In fig. 5 the output is plotted versus the delay between the switching of the prepulse and the X-ray source for different values of the PFN voltage. It is apparent that at higher PFN voltages the usable delay interval is getting smaller and smaller. At higher voltages across the laser the electron density will grow faster after preionization but in the meantime instabilities will grow causing the useable delay interval to decrease.

Fig. 6 shows the dependence of the electrical to optical efficiency on PFN charging voltage. The main efficiency is defined as optical output energy divided by the energy stored in the PFN. For the total efficiency also the energy stored on  $C_{ps}$  is taken into account. The total efficiency is best (4.6%) when the PFN is charged to 5.75 kV.

In fig. 7 electrode voltages are shown at different delays. When the X-ray source is switched at the same time as the prepulse the voltage across the peaking capacitors swings up highest. The voltage overshoot decreases when the X-ray source is switched more in advance of the prepulse. This can be explained by a decreased laser impedance at the moment the prepulse is switched.

#### 5. CONCLUSION

We have demonstrated the possibility of a reproducible high efficiency XeCl laser (4.6%) operating according the prepulse-mainpulse excitation scheme with voltage overshoot. Delay measurements have shown that the usable delay interval between switching of the X-ray source and the prepulse depends on PFN voltage. The electrical scheme is suitable for high repetition rate operation.

#### 6. ACKNOWLEDGEMENTS

The authors wish to thank H.Th.M. Prins, G.J.M. Oude Meijers, A.F. Nieuwenhuis, A.J. Braam and P. Smit for their technical support to prepare the experiments.

This work is part of the research program of the "Stichting voor Fundamenteel Onderzoek der Materie (FOM)", which is financially supported by the "Nederlandse Organisatie voor Wetenschappelijk Onderzoek (NWO)".

#### 7. REFERENCES

1. W.H. Long, M.J. Plummer, E.A. Stappaerts; *Appl. Phys. Lett.* **43**, 735 (1983)
2. C.H. Fisher, M.J. Kushner, T.E. DeHart, J.P. McDaniel, R.A. Petr, J.J. Ewing; *Appl. Phys. Lett.* **48**, 1574 (1986)
3. R.S. Taylor, K.E. Leopold; *J. Appl. Phys.* **46**, 335 (1985)
4. J.W. Gerritsen, A.L. Keet, G.J. Ernst, W.J. Witterman; *J. Appl. Phys.* **67**, 3517 (1990)

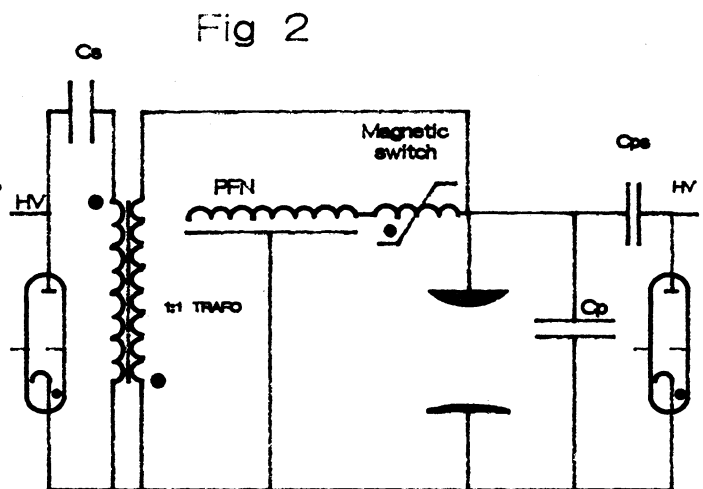
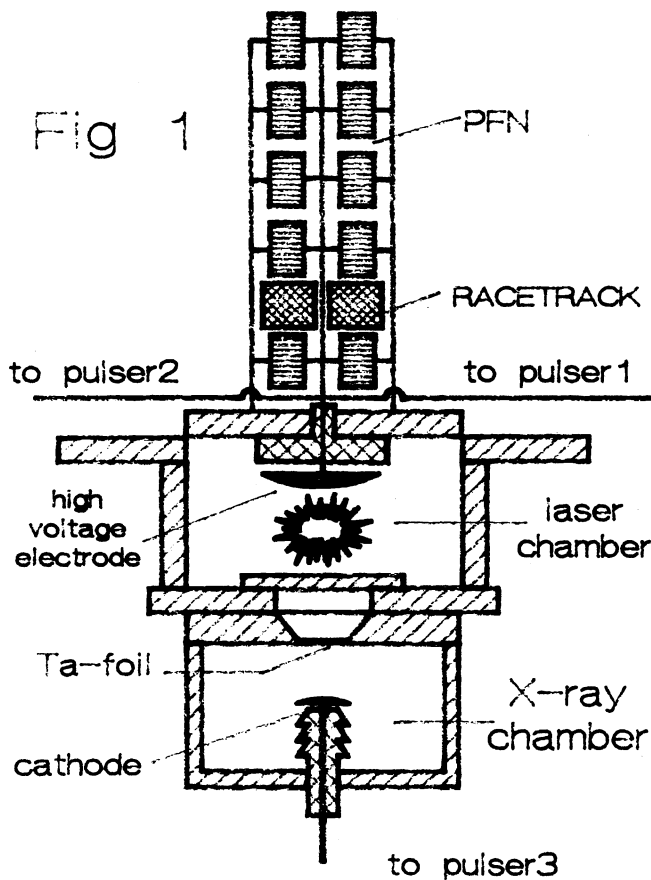


Fig. 1 Cross-sectional view of the laser including X-ray preionizer.

Fig. 2 Electrical scheme of the laser.

Fig. 3 Typical waveforms. a) Voltage across electrodes (solid) and X-ray voltage. b) Current through discharge (solid) and optical pulse.

Fig. 4 Efficiency versus partial pressure of HCl for 20 mbar of Xe and 15 mbar of Xe. Buffergas 4 bar of Neon.

Fig. 5 Output as a function of the delay between the X-ray pulse and the prepulse at 5.4 kV and 7.3 kV PFN charging voltage.

Fig. 6 Efficiency of the mainpulse alone (solid) and of mainpulse plus prepulse (dashed) as a function of PFN charging voltage.

Fig. 7 Voltage waveforms at 0 ns, 450 ns and 650 ns delay.

Fig 3a

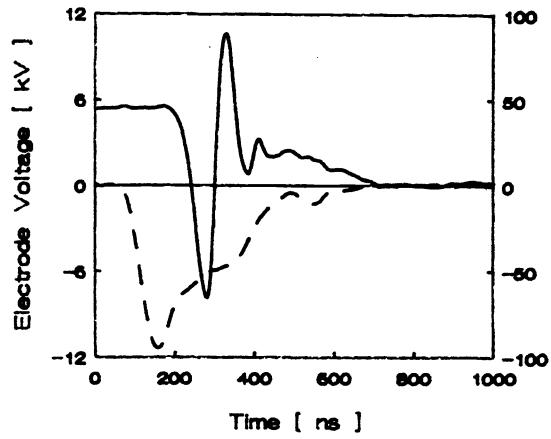


Fig 5

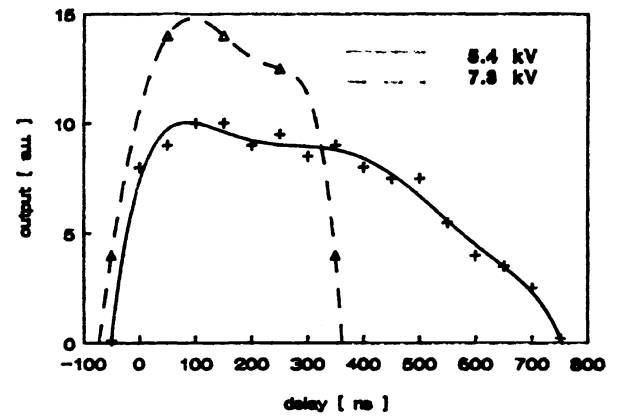


Fig 3b

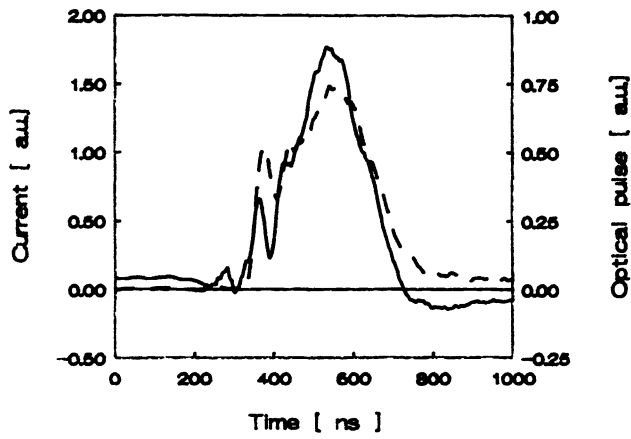


Fig 6

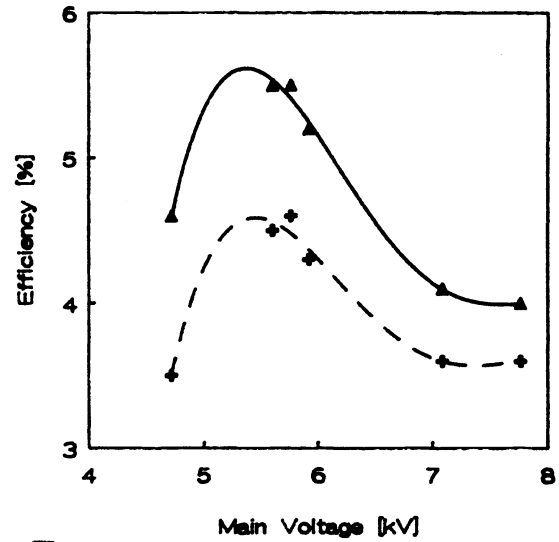


Fig 4

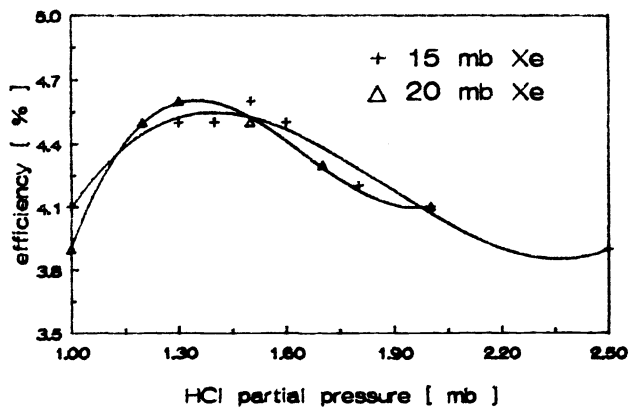


Fig 7

